Metastable eutectic in Pb-free joints between Sn-3.5Ag and Ni-based substrates

S.A. Belyakov*, C.M. Gourlay

Department of Materials, Imperial College, London SW7 2AZ, United Kingdom

Abstract:

Microstructure development in solder joints between Sn-3.5Ag and Ni-based substrates has been widely reported. However, in the present study we illustrate a new phenomenon: that during soldering of Sn-3.5Ag to Ni or ENIG (electroless nickel, immersion gold), the bulk solder solidifies to contain a metastable eutectic consisting of βSn+Ag_3Sn+$NiSn_4$ instead of the βSn+Ag_3Sn+Ni_3Sn_4, expected of equilibrium solidification. It is shown that metastable $NiSn_4$ coarsens and then decomposes into Ni_3Sn_4 and βSn during ageing at 150 and 200˚C and that coarsened $NiSn_4$ deteriorate impact shear properties.

Keywords: microstructure, intermetallic compounds, eutectic solidification, lead-free solder, electronic packaging, aging

Introduction:

Sn-3.5wt%Ag is a common solder to ENIG surface finish or Ni-based UBMs (underbump metallisations) and it is a popular choice for consumer, automotive and power electronics [1]. Various reports in the literature describe metastable Ni-Sn intermetallics (e.g. $NiSn_3$ [2-8] or $NiSn_4$ [9-14]) that form in as-reflowed [6] and thermally-cycled Sn/Ni solder joints [11], in Sn/Ni electroplated couples [2-4, 7, 8] and reaction couples under current stressing [5]. It is important to note that these metastable phases are reported to occur in the reaction layer between the solder and substrate and usually in the solid state. Recently, we have shown that metastable $NiSn_4$ also forms during eutectic solidification of binary Sn-Ni alloys [12-14]. We note that no papers report the growth of this metastable eutectic during solidification of industrially-important solder-substrate combinations. For example, in the case of Sn-3.5Ag joints on Ni-based substrates, βSn grain microstructure and its evolution during thermal loading are widely reported [15, 16], and a large body of research has been devoted to the interfacial reactions between Sn-3.5Ag and ENIG substrates during solder joint manufacturing and during ageing

at elevated temperatures [15-18]. However, no reports describe metastable $NiSn_4$ phase formation in these systems during solidification. Since there is negligible solubility of Ni in Ag_3Sn and βSn [15, 19], it is likely that Ni dissolved from the substrate will form Ni_xSn_y intermetallic in the bulk solder in addition to in the interfacial layer. Therefore, it seems surprising that past work has not reported on Ni_xSn_y intermetallics in the bulk solder and whether they are stable Ni_3Sn_4 or metastable $NiSn_4$/$NiSn_3$. The aims of the present study were (i) to explore whether metastable $NiSn_4$ forms during the solidification of industrially-important Sn-3.5Ag/Ni or /ENIG solder joints and, if so to (ii) investigate the decomposition of metastable $NiSn_4$ during artificial ageing.

Experimental Methods:

Ni and ENIG-coated Cu substrates were produced from 0.5mm thickness sheet of 99.9Ni or 99.9Cu. ENIG plating yielded a ~5µm Ni-P layer (16at%P) and a 0.06 µm Au layer. Coupons of 10 x 10 mm were cut from the sheets and 100µm Sn-3.5Ag solder preforms were placed on the substrates above RM5 flux cream. Reflow soldering was conducted with a heating rate of 1 K/s, time above Sn-Ag eutectic temperature of ~80 s, peak temperature of 250°C and a cooling rate of 3 K/s. Joints were subjected to solid-state heat treatments at 150°C and 220°C for up to three months. Microstructure characterisation was conducted in a Zeiss Auriga scanning electron microscope with an INCA x-sight energy dispersive X-ray (EDX) detector and Bruker electron backscattered diffraction (EBSD) detector.

Results and Discussion:

Figure 1 shows a typical cross-section from a Sn-3.5Ag/Ni joint at a range of magnifications. Figure 1A is a schematic of the whole joint for scale. Figure 1B is from an area similar to the rectangle in Figure 1A. A Ni_3Sn_4 -layer is present at the interface with the Ni substrate and the microstructure in the bulk solder is comprised of βSn dendrites surrounded by a eutectic mixture. Note that the βSn matrix has been selectively etched from the surface to improve the imaging of the eutectic morphology. Figures 1C and 1D depict the eutectic region in more detail. Two distinct morphologies can be differentiated: (i) rod-like and (ii) sheet-like eutectic phases. With EDX, the rod-like eutectic phase was found to correspond to Ag_3Sn and the sheet-like eutectic phase has the composition close to $NiSn_4$ (Table 1).

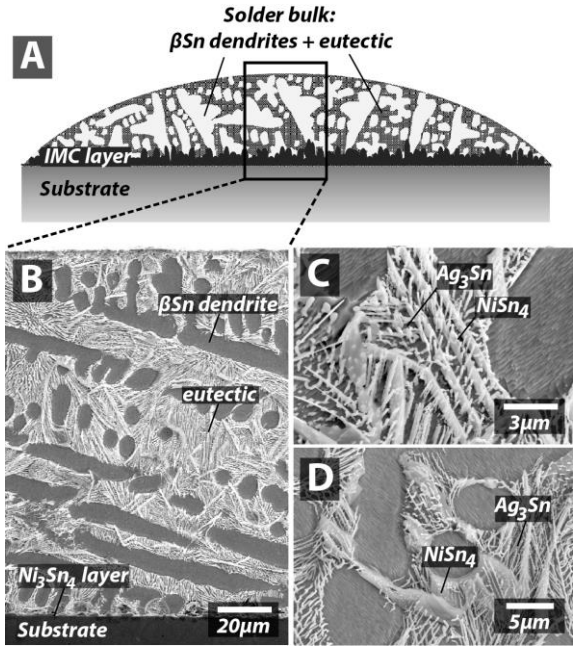

Figure 1. (A): schematic solder joint cross-section, (B,C,D): microstructures of as-soldered Sn-3.5Ag/Ni joints at different magnifications, βSn was selectively removed.

Table 1. SEM-EDX measurements of the eutectic intermetallics in as-soldered Sn-3.5Ag/Ni and Sn-3.5Ag/ENIG solder joints.

	Sn, at%	Ni, at%	Au, at%	Ag, at%	Proposed phase
Sn-3.5Ag/Ni solder joints					
Mean	81.2	18.8	-	**-**	**$NiSn_4$**
St. dev.	0.78	0.78	-	-	
Mean	24.9	-	-	75.1	**Ag_3Sn**
St. dev.	0.56	-	-	0.56	
Sn-3.5Ag/ENIG solder joints					
Mean	81.9	12.3	5.8	**-**	**$(Ni,Au)Sn_4$**
St. dev.	0.94	0.94	1.34	-	
At least 10 particles were measured for each phase					

The identity of the intermetallics was further confirmed by EBSD, where the $NiSn_4$ EBSD patterns (Figure 2B) could only be indexed as o*C*20-$NiSn_4$ phase (Figure 2D), consistent with $NiSn_4$ being isomorphous to $PdSn_4$, $PtSn_4$ and $AuSn_4$ [20]. Note that the $NiSn_4$ has a very similar sheet-like morphology to the eutectic $NiSn_4$ in binary Sn-Ni alloys [12, 13]. Table 1 also shows no Ag solubility in $NiSn_4$ and no Ni was detected in Ag_3Sn. Examination of microstructures revealed that some eutectic

regions contained only βSn + Ag_3Sn whilst others contained βSn + Ag_3Sn + $NiSn_4$. Since this is three-component solidification, it can be inferred that the solidification sequence was: (i) L → βSn primary dendrite growth (Figure 1B), followed by (ii) L → βSn + Ag_3Sn univariant eutectic growth and finally (iii) L → βSn + Ag_3Sn + $NiSn_4$ invariant eutectic growth; i.e. the $NiSn_4$ formed in a ternary eutectic reaction during the latest solidification stages.

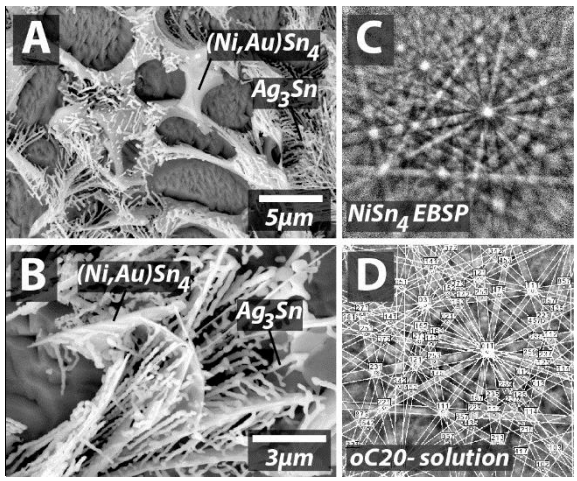

Figure 2. Eutectic microstructures of as-soldered (A,C) Sn-3.5Ag/ENIG joints, βSn was selectively removed; (B): representative EBSP from $NiSn_4$ eutectic and (D): solution of EBSP in (B) as oC20-$NiSn_4$.

Figures 2(A) and (B) show typical eutectic regions in as-soldered Sn-3.5Ag/ENIG joints. Similar to soldering to Ni, there are two distinct intermetallic phases in the eutectic: a rod-like and a sheet-like phase. The EDX results in Table 1 show that the sheet-like phase has composition consistent with (Ni,Au)Sn_4 and contains approximately twice as much Ni as Au. EBSD patterns similar to Figure 2(C) could only be indexed as o*C*20-$NiSn_4$ or isotypic $AuSn_4$, $PdSn_4$ or $PtSn_4$. The presence of Au in Sn-3.5Ag/ENIG solder joints added extra complexity to the system. The EDX results in Table 1 suggest that most dissolved Au segregated to $NiSn_4$ because no Au was detected in the βSn matrix, Ag_3Sn or Ni_3Sn_4 interfacial layer. The volume fraction of $NiSn_4$ eutectic sheets was noticeably higher in Sn-3.5Ag/ENIG than Sn-3.5Ag/Ni joints as dissolved Au atoms replaced Ni atoms in the $NiSn_4$ phase up to 6% (Table 1). Other than the increased volume fraction of $NiSn_4$ eutectic, no major differences were observed for 3.5Ag/Ni and 3.5Ag/ENIG solder joint bulk microstructures. The interfacial zone in ENIG-plated

solder joints contained multiple layers but with Ni_3Sn_4 as the intermetallic on the Sn side, which is consistent with past literature [15, 16].

$NiSn_4$ is not an equilibrium phase in the Sn-Ag-Ni system [21] and it was found here that $NiSn_4$ undergoes the following transformation $NiSn_4 \rightarrow Ni_3Sn_4 + \beta Sn$ with time at 150 and 200°C. Figure 3 (A-B) demonstrates the microstructural changes during ageing of Sn-3.5Ag/Ni joints at 150°C. It was found that $NiSn_4$ decomposition in Sn-3.5Ag/Ni joints occurs in two stages: (i) coarsening of eutectic $NiSn_4$ sheets into tile-like $NiSn_4$ particles up to 20µm in size, similar to that shown in Figure 3C, followed by (ii) $NiSn_4 \rightarrow Ni_3Sn_4 + \beta Sn$ decomposition. Typical, newly formed Ni_3Sn_4 crystals are shown in Figure 3D.

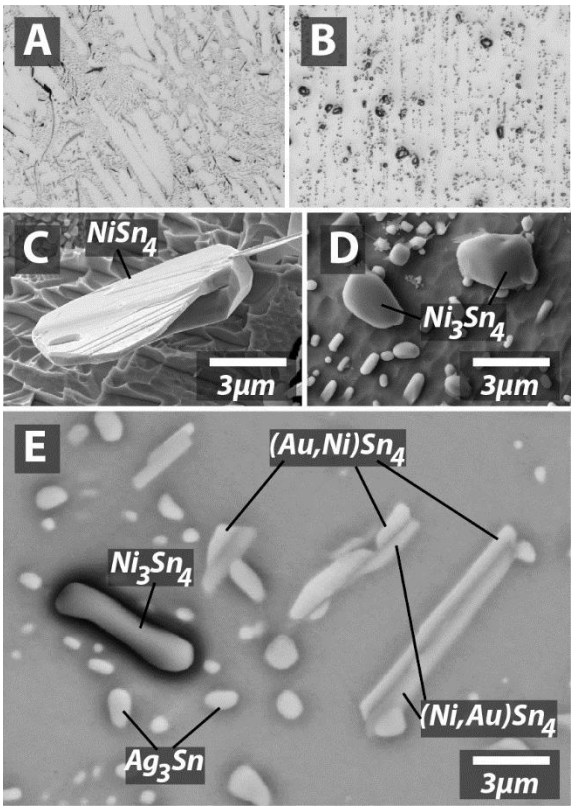

Figure 3. Sn-3.5Ag/Ni solder joint (A): as-soldered and (B): heat treated 1 month at 150°C. (C): coarsened $NiSn_4$ eutectic particle and (D): Ni_3Sn_4 crystals formed during $NiSn_4 \rightarrow Ni_3Sn_4 + \beta Sn$ transformation. (E): BSE image depicting $(Ni,Au)Sn_4 \rightarrow Ni_3Sn_4 + AuSn_4 + \beta Sn$ transformation during ageing of Sn-3.5Ag/ENIG joints at 150°C

The presence of Au in Sn-3.5Ag/ENIG joints added extra complexity in the $NiSn_4$ decomposition process. Figure 3E shows that, during ageing at 150°C, the Au separates from coarsening $(Ni,Au)Sn_4$ particles to form $(Au,Ni)Sn_4$ attached to the $(Ni,Au)Sn_4$. As the Au content of $(Ni,Au)Sn_4$ decreases, it then transforms into Ni_3Sn_4. In the backscattered electron image of Figure 3E Au-rich $(Au,Ni)Sn_4$ is brighter than Ni-rich $(Ni,Au)Sn_4$ and Ni_3Sn_4 is the darkest phase. Further micrographs showing microstructure evolution during $(Ni,Au)Sn_4$ decomposition are given in Supplementary Information Figures SI 2-3. After $NiSn_4$ transformation, $AuSn_4$ shortly existed in the bulk as tile-like crystals measuring up to ~2μm in size that then disappeared during prolonged ageing. It is feasible that the Au dissolved into the βSn matrix as, according to the Sn-Au phase diagram [22], βSn can dissolve up to 0.28-0.4wt%Au at the ageing temperatures (150-200°C), which is above the amount of Au dissolved from the 60nm Au layer during soldering. A number of authors [23-25] report on $AuSn_4$ reprecipitation in the interfacial zone during ageing. This was not observed in the current investigation after three months at 150°C or 200°C, most likely because the Au capping layer on the ENIG used was much thinner than in [23]. The transformation of $NiSn_4$ or $(Au,Ni)Sn_4$ eutectic did not go to completion at 150°C in the 3 month time frame of the present study, indicating that decomposition would depend on the working environment of a solder joint and it is highly likely to be ongoing throughout its life. Further work is required to quantify the decomposition kinetics.

Given that joints between Sn-3.5Ag and ENIG have been in widespread industrial use for many years and there are many scientific papers on this solder-substrate combination (e.g. [15-18]), it is surprising that metastable $NiSn_4$ in the eutectic has not been reported before. One reason may be the difficulty of observing the thin $NiSn_4$ eutectic sheets in polished cross-sections- we find that selective etching of βSn (such as in Fig.1 and 2) is useful in clearly revealing the eutectic intermetallics. Another reason may be that the presence of Au has clouded the interpretation, with researchers assuming this is $AuSn_4$ with some dissolved Ni. However, our findings of eutectic $NiSn_4$ when Sn-3.5Ag is soldered to Ni demonstrates that Au is not necessary for $NiSn_4$ to form The nucleation and growth advantages of

metastable $NiSn_4$ over stable Ni_3Sn_4 are likely to be similar to those discussed previously for the binary Ni-Sn system [12].

Since $NiSn_4$ grows in a eutectic reaction, it is distributed throughout the whole of the bulk solder (e.g. Figure 1(B)). It is, therefore, natural to ask how metastable $NiSn_4$ and its decomposition to stable Ni_3Sn_4 influence joint reliability. Figure 4 shows results of impact shear testing of 500µm Sn-3.5Ag-0.1Ni solder balls on ENIG substrates. The shear test displacement rate was 100mm/s. It can be seen that coarsened $NiSn_4$ particles are on the fracture surface indicating that $NiSn_4$ was involved in crack nucleation and/or propagation. Coarsened $NiSn_4$ particles seem to act similar to the widely reported embrittlement of solder joints by isomorphous $AuSn_4$ or $PdSn_4$ phases [24, 26-28].

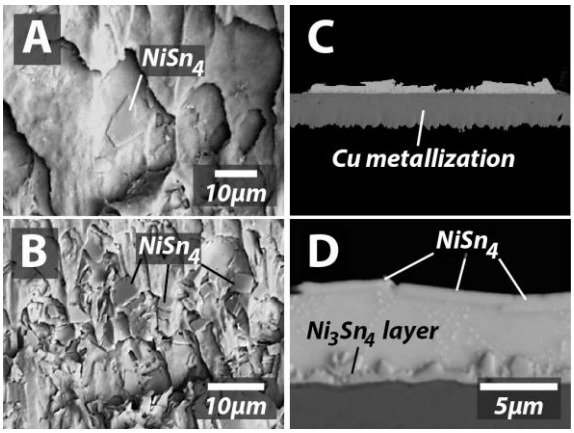

Figure 4. Fracture surfaces of 500 µm Sn-3.5Ag-0.1Ni solder balls soldered to ENIG. (A), (B): view from above and (C), (D): side view featuring coarsened $NiSn_4$ particles. Ageing conditions: 1 month at 150°C.

Conclusions:

In summary, where previous research on Sn-3.5Ag/ENIG joints report only the equilibrium phases growing in the system, it has been shown here that the bulk solder solidifies to contain a metastable eutectic consisting of $\beta Sn+Ag_3Sn+NiSn_4$ instead of the expected $\beta Sn+Ag_3Sn+Ni_3Sn_4$. Metastable $NiSn_4$ has been found to coarsen and then decompose into stable Ni_3Sn_4 during ageing at 150°C and this reaction did not go to completion in 3 months. Additionally, coarsened $NiSn_4$ was found on the

fracture surface after impact shear testing. These findings point to the need to develop approaches to control eutectic $NiSn_4$ formation, coarsening and decomposition.

Acknowledgements

This research was funded by Nihon Superior Co., Ltd. and UK EPSRC grant EP/M002241/1

References:

1. B.T. Zhou, G. Muralidharan, K. Kurumadalli, C.M. Parish, S. Leslie, T.R. Bieler, J. Electron. Mater. 43 (2014) 57.
2. P.J. Kay, C.A. Mackay, Trans. Inst. Met. Finish. 54 (1977) 68.
3. J. Haimovich, Weld. J. 68 (1989) S102.
4. J. Haimovich, D. Kahn, 77th AESF Annual Technical Conference. 1990. Boston.
5. C.M. Chen, S.W. Chen,. J. Mater. Res. 18 (2003) 1293.
6. W.K. Choi, H.M. Lee, J. Electron. Mater. 28 (1999) 1251.
7. I. Vitina, I. Pelece, V. Rubene, V. Belmane, M. Lubane, A. Krumina, Z. Zarina et al.. Sci. Technol., 11 (1997)835.
8. W. Zhang, M. Clauss, F. Schwager, IEEE Trans. Compon., Packag., Manuf. Technol. 1 (2011) 1259.
9. C.H. Wang, C.Y. Kuo, H.H. Chen, S.W. Chen, S. W., Intermetallics 19 (2011) 75.
10. L.J. Zhang, L. Wang, X.M. Xie, W. Kempe., 5th Int. IEEE Symp., Shanghai, 2002
11. W.J. Boettinger, M.D. Vaudin, M.E. Williams, L.A. Bendersky, W.R. Wagner, J. Electron. Mater., 32 (2003) 511.
12. S.A. Belyakov, C.M. Gourlay, Intermetallics. 25 (2012) 48.
13. S.A. Belyakov, C.M. Gourlay, J. Electron. Mater. 41 (2012) 3331.
14. S.A. Belyakov, C.M. Gourlay, Intermetallics, 37 (2013) 32.
15. J.W. Yoon, H.S. Chun, S.B. Jung, J. Mater. Sci.: Mater. Electron. 18 (2007) 559.
16. J.W. Yoon, B.I. Noh, S.B. Jung, IEEE Trans. Compon., Packag., Manuf. Technol. 33 (2010) 64.
17. Y.B. Park, B.R. Lee, J.M. Kim, Korean J. Mater. Res., 24 (2014) 166.
18. Y. Yang, J.N. Balaraju, Y. Huang, Y. Tay, Y. Shen, Z. Tsakadze, Z. Chen, J. Electron. Mater. 43 (2014) 4103.
19. C. Schmetterer, C. Flandorfer, H. Richter, K. W. Saeed, U. Kauffman, M.P. Roussel, H. Ipser, Intermetallics, 15 (2007) 869.
20. S.A. Belyakov, C.M. Gourlay, Acta Mater. 71 (2014). 56.
21. C. Schmetterer, H. Flandorfer, H. Ipser, Acta Mater. 56 (2008) 155.
22. H. Okamoto, Phase diagrams of dilute binary alloys. ASM International, Materials Park, 2002
23. T. Laurila, V. Vuorinen, Mater. 2 (2009) 1796.
24. Z.Q. Mei, M. Kaufmann, A. Eslambolchi, P. Johnson, E. Eia, IEEE 48th Electronic Components & Technology Conference. 1998. New York.
25. A.M. Minor, J.W. Morris, Metall. Mater. Trans. A. 31 (2000) 798.
26. M.O. Alam, B.Y. Wu, Y.C. Chan, L. Rufer, IEEE Trans. Device Mater. Reliab. 6 (2006) 421.
27. X.J. Huang, S.W.R. Lee, M. Li, W.T. Chen, IEEE 54th Electronic Components & Technology Conference, 2004. New York.
28. C.E. Ho, W.H. Wu, C.C. Wang, Y.C. Lin, J. Electron. Mater. 41 (2012) 3266.